Evaluation of X-ray Diffraction Data from Protein Crystals by Use of an Imaging Plate

By Isao Fujii, Yukio Morimoto, Yoshiki Higuchi and Noritake Yasuoka

Department of Life Science, Faculty of Science, Himeji Institute of Technology, Shosha 2167, Himeji 671-22, Japan

Chuuji Katayama

MAC Science, Nakanouemati 2-25-6, Hachiouji 192, Japan

and Kunio Miki

Department of Applied Chemistry, Faculty of Engineering, Osaka University, Yamadaoka 2-1, Suita, Osaka 565, Japan

Abstract

A system has been developed which uses an imaging-plate diffraction apparatus to obtain structure factors for protein crystals. The latter is connected to a graphics workstation through an Ethernet. Pixel data from an imaging plate are transferred *via* the Ethernet to a workstation and processed to give the structure factors. The quality and precision of the diffraction data were examined from the point of view of spatial uniformity, linearity with exposure, decay with time, and reproducibility. X-rays from an ^{55}Fe source and Debye–Scherrer rings from Si powder were used for calibration purposes. Finally, diffraction data were obtained and evaluated for lysozyme and cytochrome c-553 using this system. The results were satisfactory in terms of sensitivity and precision.

Introduction

The usefulness of imaging plates in X-ray diffraction experiments has been recognized increasingly in many fields. Miyahara, Takahashi, Amemiya, Kamiya & Satow (1986) used imaging plates, originally developed for diagnostic radiography, as a new integrating area detector, and described fundamental performance features such as spatial resolution, uniformity and so on. The advantages of imaging plates compared with other integrating detectors such as X-ray films and X-ray TV detectors are obvious, especially in protein crystallography where specimens often suffer from radiation damage. We have introduced an imaging-plate detector system in our laboratory, and developed a through-processing system from X-ray exposure to structure-factor data. The efficiency and precision of the system are satis-

factory for the purposes of protein crystallography, as reported in this paper. Sakabe, Nakagawa, Sasaki, Sakabe, Watanabe, Kondo & Shimomura (1989) have demonstrated the usefulness of imaging plates in combination with Weissenberg photography for protein crystallography, in work at the Photon Factory.

System description

The system consists of three components: (i) an X-ray generator (RU300, Rigaku); (ii) an integrating area detector using an imaging plate (DIP100, MAC Science); (iii) a graphics workstation (TITAN, Kubota) equipped with two cpu's, R2000 (24 MIPS), memory 64 MB and a color display.

It is worth mentioning some of the details of the process used to obtain the X-ray exposed imaging plate and evaluate the diffraction data. The DIP100 experimental setup is illustrated in Fig. 1. A rotating-anode X-ray generator operated in fine-focus mode (focus 0·3 × 3 mm) and a collimator (150 mm long) with double holes (0·5 mm diameter) in order to minimize the incident-beam divergence relative to the specimen (which would make spatial resolution worse) were used.

An imaging plate (200 mm in diameter) covered with a photostimulable phosphor ($BaFBr:Eu^{2+}$, 0·15 mm in thickness) (Miyahara & Kato, 1984; Takahashi, Miyahara & Shibahara, 1985) was used. A two-dimensional X-ray image obtained from a specimen crystal is stored as a distribution of *F* centers. The diffraction pattern is then read by measuring the fluorescence intensity stimulated by a focused He–Ne laser beam scanning the surface of the phosphor screen. At the read-out stage, a reader

head traverses an imaging plate rotated at a fixed speed (391 r.p.m.) in a similar manner to a record playing on a phonograph. The process is illustrated in Fig. 2. This mode of scanning, as opposed to raster scanning, needs some corrections or calibrations to be applied to the intensities thus obtained. This will be discussed later. After an X-ray image has been read, the surface of the imaging plate is illuminated with filtered strong light in order to completely erase the remaining stored image so that the next exposure can be recorded. The photostimulated luminescence thus released is collected by two photomultiplier tubes, one for the stronger region and the other for the weaker region, in order to retain a wide dynamic range. The output signals from the photomultiplier tubes are converted into digital values along a spiral path, as shown in Fig. 2(*a*), and are stored in a mass memory. These values are then converted into pixel data in a rectangular coordinate system (Fig. 2*b*) after multiplying by geometrical factors to take account of the non-uniform interval resulting from the spiral scanning mode. The intensity for each rectangular pixel is expressed in 16 bits. The pixel size is designed to be $125 \times 125 \, \mu m$, and 1600×1600 pixels are sufficient to cover an imaging plate of 200 mm diameter (Fig. 2*b*). To store pixel data in each frame of an imaging plate requires 5 MB. Data transfer by the direct memory access mode is used in order to minimize the time required.

Data-processing strategy

A series of operations are needed to derive pixel data for each frame of an imaging plate. For example, to obtain a still photograph of a protein crystal, the following operations are necessary: erase the imaging plate, rotate the crystal about the spindle axis to obtain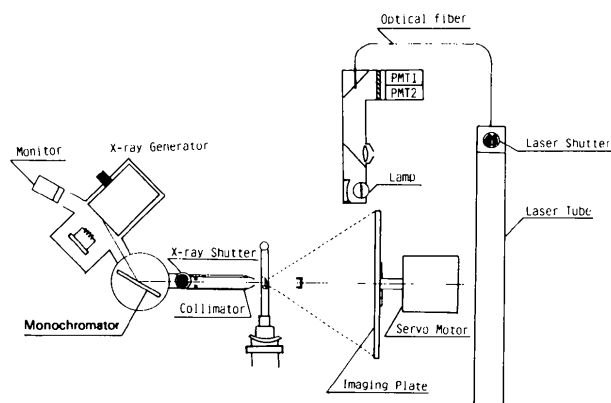 the required angle, open the X-ray shutter for the desired length of time, close the shutter, read out the photostimulated luminescence, convert the data to intensities for each pixel. In order to make the operations easier on the DIP100, we have developed some control programs describing just such a series of instructions. The programs have been developed as console commands in the C language. Some of these console commands and their functions are summarized in Table 1.

A typical strategy for obtaining diffraction data for a protein crystal is now described. A crystal is mounted on a spindle axis, and a still photograph taken using the *STILL* command. The horizontal or vertical distance between the center of the frame and the center of the corn and the goniometer arcs and spindle axis adjusted according to the usual alignment procedures. After alignment of the crystal, a series of oscillation photographs are taken for a specified oscillation angle. Still photographs are taken before and after each oscillation photograph. This procedure is used because the data are processed by the program *FILME* which was originally developed by Schwager, Bartels & Jones (1975) and
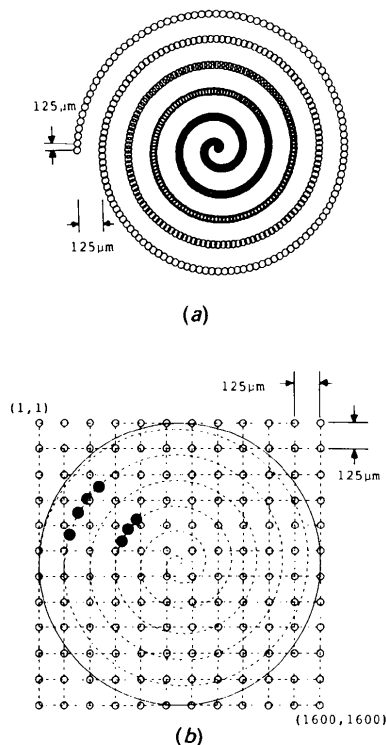

(*a*)

(*b*)

Fig. 2. Schematic representation of the scanning mode. (*a*) Conversion of the output signals to digital values. (*b*) Conversion of digital values to pixel data after multiplying by geometrical correction factors (as indicated by a number of ● marks in the matrices) to take account of the non-uniform interval resulting from the spiral scanning mode. This correction is carried out at the next stage by the program *OSCONV*.

Fig. 1. Experimental setup of DIP100.

Table 1. *Console commands and their functions*

INIT	Initialize the DIP100 controller, load the coordinate transfer table and erase an imaging plate. Usually 60 min is needed for warm-up when this system is used for quantitative measurement.
OSC	Take an oscillation photograph; set an oscillation range, exposure time and repetition times, and carry out X-ray exposure.
STILL	Take a still photograph; set a spindle axis at the specified angle and exposure time, and carry out X-ray exposure.
ERASE	Initialize an imaging plate.
TITAN	Transfer pixel data to a TITAN workstation *via* the Ethernet.
DISP	Display a diffraction image on a CRT, and make a hard copy if wanted.

Jones, Bartels & Schwager (1977) and adapted for TITAN by us.

The pixel data are transferred to a TITAN workstation *via* the Ethernet. The procedure used to obtain structure-factor data from a series of pixel data for the subsequent frames of still and oscillation photographs is illustrated in Fig. 3. Leading zeros in the data are suppressed in order to give a compressed form and hence save auxiliary storage. *STCONV* or *OSCONV* converts compressed data back to pixel data in order to obtain still or oscillation photographs.
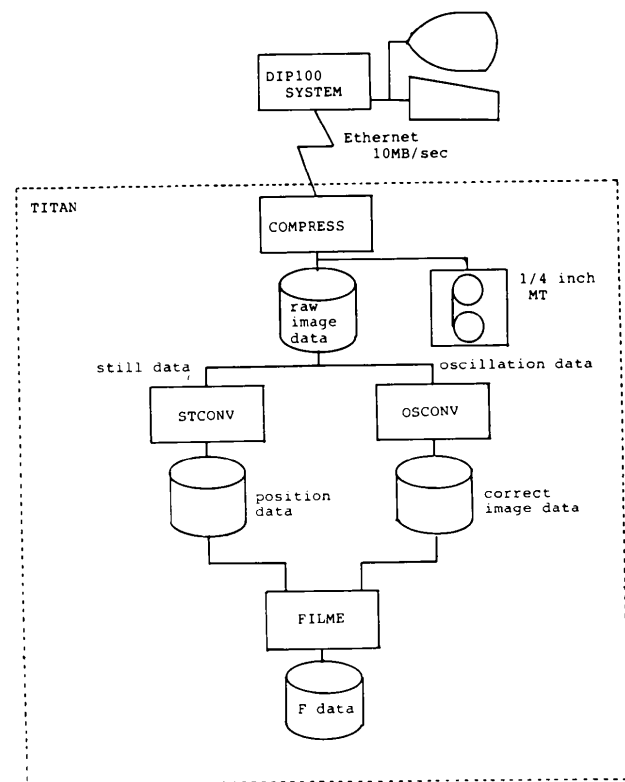

Fig. 3. Processing of the image data. The recorded frames are transferred into the TITAN workstation and compressed in order to save memory space. The preprocessing programs *STCONV* and *OSCONV* convert pixel data in each frame into manageable data for the indexing program *FILME*.

The preceding and succeeding still photographs are used to refine the orientation matrices for the reciprocal lattice. It takes about 7 min to process an oscillation photograph, to obtain structure factors, and to evaluate some statistical values such as the symmetrical reliability factor, for example.

The following points may be made concerning the program *FILME* as modified for use on our system.

(i) The pixel size, originally designed to be 50 or 100 μm per raster has been modified to 125 μm.

(ii) The record size used to express the intensity of a pixel has been changed from 1 byte to multibyte.

(iii) Dimensions have been expanded in order to deal with the large number of pixels corresponding to a wide area.

(iv) The program, originally written in a sophisticated manner so as to store many steps of instructions and a large number of data, has been rewritten in a simpler form by use of the virtual-memory-programming technique. This allows the revised program to process faster.

(v) The *X-Window* system has been introduced to control the sequence of jobs which process the pixel data to give structure factors. This enables semi-realtime processing.

(vi) A picture corresponding to the original diffraction or simulated pattern is easily and quickly displayed on a graphics workstation.

These modifications together with the *X-Window* utility provide a more user-friendly environment in which to process diffraction experiments.

Examination of the performance of the system

Sensitivity of the imaging plate

The sensitivity should be uniform over the whole area of the imaging plate. In order to check this, the following experiment was carried out. Equal exposure was given to three points on an imaging plate using radioisotope ^{55}Fe (30 μCi). The number of photons was increased with increasing exposure time. The points were 93·6, 63·5 and 36·2 mm from the center of the imaging plate. In addition, the absolute value of the intensity of the radioisotope was measured with a scintillation counter. The results are shown in Fig. 4. It is noteworthy that the measured intensity has almost the same value up to $2\cdot5 \times 10^6$ photons while some discrepancies are clearly recognized in the high-intensity region. This effect may be due to the spiral scanning mode which means that the scan speed is lower in the inner part of the imaging plate.

In order to examine the spatial deviations in intensity, the following experiment was carried out: equal exposure was given along concentric circles by rotating the imaging plate, and the intensities read

at 20 points. The average value and standard deviations obtained are plotted in Fig. 5. This shows the deviations are due to random errors and no systematic errors are present.

Linearity

The Debye–Scherrer rings from Si powder were used to check the linearity of the imaging plate. The measured intensities are plotted against exposure time in Fig. 6. This shows the wide-ranging linearity of the system, up to 10^5 at least.

Stability

Measurement of the intensity of powder diffraction of Si is repeated after a specified interval. The results are shown in Fig. 7. The fluctuation of each measurement is within the range of the statistics.

Observed decay of the F centers

It is well known that F centers produced by X-rays decay with time. In order to check this phenomenon, the intensity diffracted by a graphite plate was measured repeatedly, varying the time between exposure and measurement. The results are shown in Fig. 8. It is noteworthy that the low temperature is useful in preventing the decay of the F centers. The curve shown in Fig. 8 could not be fitted with a single exponential function, but can be expressed as:

$$I(t) = I_1 \exp(-\lambda_1 t) + I_2 \exp(-\lambda_2 t) \qquad (1)$$
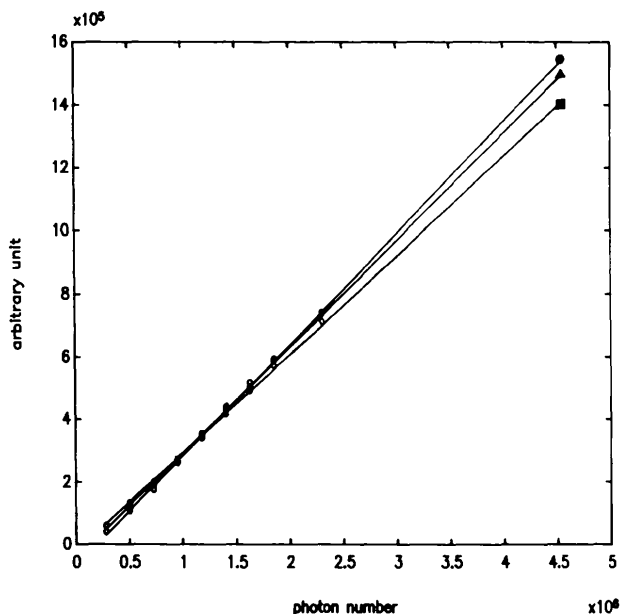
where $I_1 + I_2$ is the given exposure, λ_1 and λ_2 are constants concerning the decay mechanism, and t is the time between exposure and measurement. This observation strongly suggests that decay of the F centers is due to two different processes, and this problem remains unresolved.
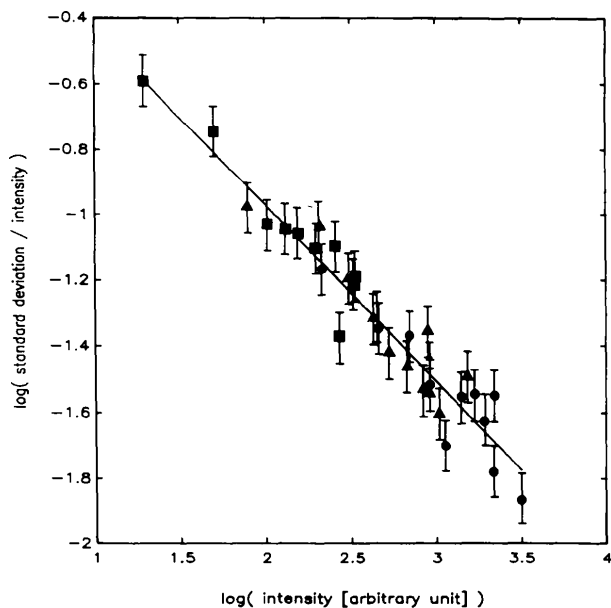

Fig. 5. Reliability of the imaging plate. Equal exposure was given along concentric circles by rotating the imaging plate, and the intensities read at 20 points along a circle. The average value and standard deviations obtained are plotted at radii 80 (●), 100 (▲) and 120 mm (■) from the center of the imaging plate. The error bars indicate the standard deviation of each point from the line fitted by the least-squares method.
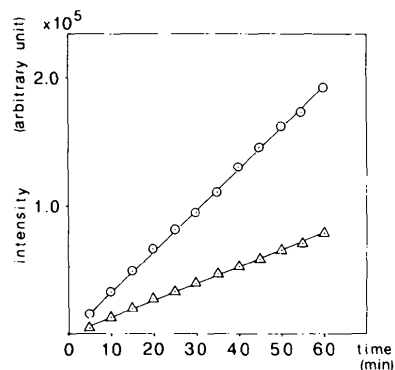

Fig. 4. Sensitivity of the imaging plate. The calibrated radio-isotope ^{55}Fe (30 μCi) gives the same amount of exposure to the points 93·6 (■), 63·5 (▲) and 36·2 mm (●) from the center of an imaging plate.

Fig. 6. Si powder diffraction. The Debye–Scherrer rings from Si powder were used to check the linearity of the imaging plate. The measured intensities are plotted against time of exposure. Data for rings (111) (○) and (220) (△) are summed over the circumference without correction. This shows the linearity of the system at high intensities (up to 10^5 at least).

Correction curve for the spiral scanning mode

As already mentioned (see Fig. 2), because of the spiral scanning mode it is most important to find a good calibration procedure. In order to find a functional form for the calibration, we carried out the following experiment. A uniform exposure was made along a radius of an imaging plate using the radioisotope ^{55}Fe (30 μCi). The latter was mounted on the reader head and traversed repeatedly at lower speed, say 100 mm min^{-1}, for specified times, and the intensity along a radius read off. The data obtained are plotted in Fig. 9(a). This curve shows that the spiral scanning mode gives outer pixels apparently stronger intensities, and the correction function should therefore be one which is inversely proportional to the curve obtained here. The ratios of each curve to the one for largest exposure (600 min) are given in Fig. 9(b), and it is clear that the correction curve is independent of exposure. The correction function is therefore obtained using the largest exposure data.

Many kinds of functions were proposed based on the mechanism of observation, but it is not so easy to derive an appropriate functional form on the basis of simple theory. However, a good fit is obtained using the following function:

$$I(r) = kr/(r + a) \qquad (2)$$

where $I(r)$ is the intensity at a distance r from the center of an imaging plate, and k and a are constants. This function is satisfactory for calibration of the spiral scanning mode as shown in Fig. 10.

(a)

(b)
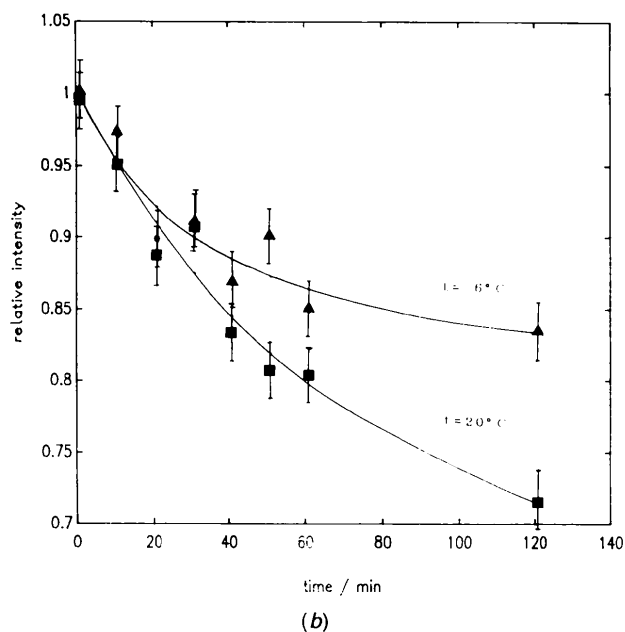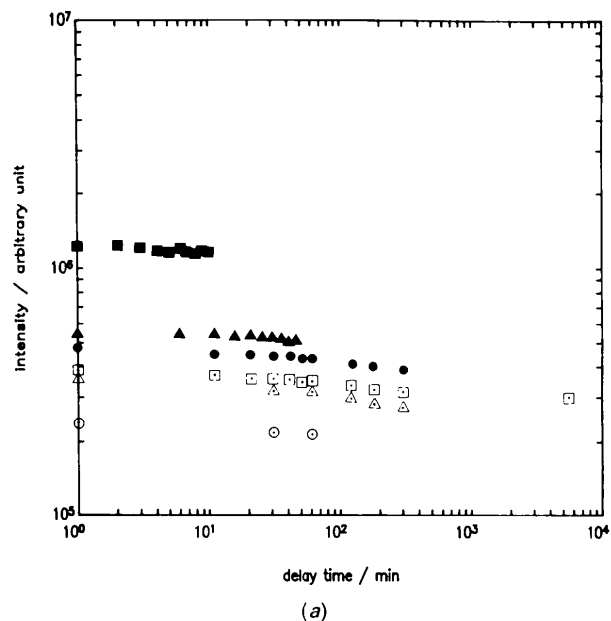
Fig. 8. Decay of an exposed imaging plate. (a) The various intensities diffracted by a graphite plate were measured repeatedly, varying the time between exposure and measurement. The symbols ■ and ▲ indicate data measured at a radius of 55·0 mm, and symbols □, △ and ○ at 45·0 mm. Typical features are observed in the decay curves. (b) Data sets shown at 279 (1) and 293 (4) K for a radius of 95·6 mm. The intensities were normalized to the first set of data. The parameters I_1, λ_1, I_2 and λ_2 are 0·904, 6·74 × 10^{-4}, 0·105 and 8·49 × 10^{-2} at 279 K. At 293 K the respective values are 0·909, 1·97 × 10^{-3}, 0·107 and 0·150.
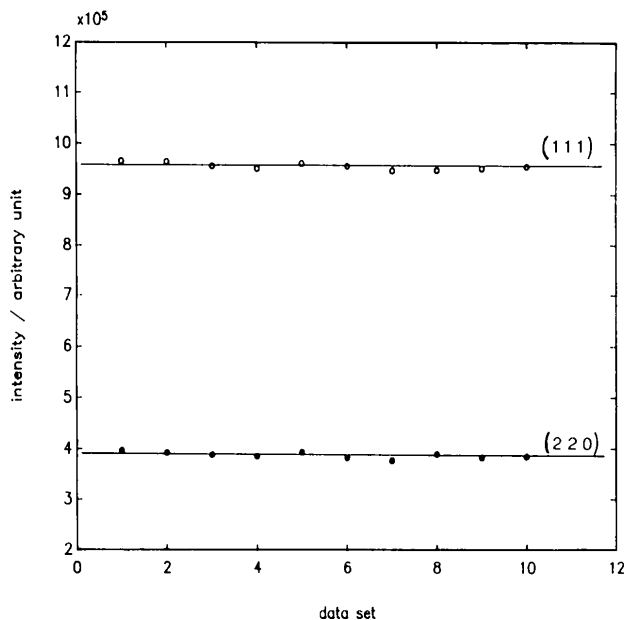

Fig. 7. Stabilization of the system. Intensities of the Debye–Scherrer rings from Si powder were measured for 30 min exposures with a 1 h interval. The data for rings (111) and (220) are summed over the circumference without correction. The fluctuation of each measurement is within the range of the statistics.

Examples of data collection for protein crystals using the imaging system

In order to explore the optimum conditions for data collection on a protein crystal, diffraction experiments have been carried out on hen egg lysozyme. Experimental conditions and statistics of data obtained are summarized in Table 2. Two sets of data have been collected. Oscillation of the crystal was not repeated for DATA(I) of Table 2, while it was repeated five times for DATA(II). The total number of reflections is greater for DATA(I) than for DATA(II), whereas the number of rejected reflections is greater for DATA(I). Rejected reflections are those for which the difference between symmetrically equivalent reflections is greater than 30%. Comparison of the two data sets suggests that repeated oscillations are necessary in spite of their effect on partial reflections. This may be due to decay of the F centers (see Fig. 8). The time taken to collect each data set was approximately 12 h.

In order to assess the performance of this imaging-plate diffraction system, reflection data for a lysozyme crystal were also collected using a four-circle diffractometer. The results are listed in Table 2. These data are considered to be of similar quality.

Another diffraction experiment has been carried out using a cytochrome c-553 crystal obtained from sulfate-reducing bacteria (Nakagawa, Nagashima, Higuchi, Kusunoki, Matsuura, Yasuoka, Katsube, Chihara & Yagi, 1986). The results are summarized in Table 3. It took 28 h to obtain two sets of data at 2·3 Å resolution, which were of higher quality.

Discussion

A method of obtaining structure-factor data for protein crystals using an imaging-plate diffraction
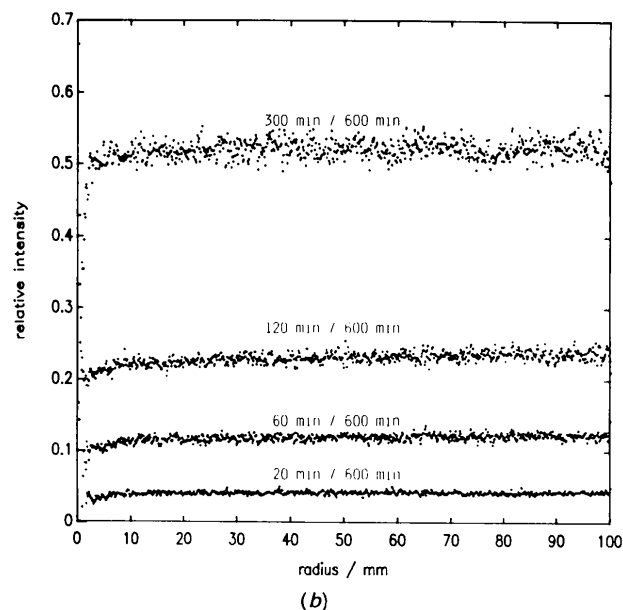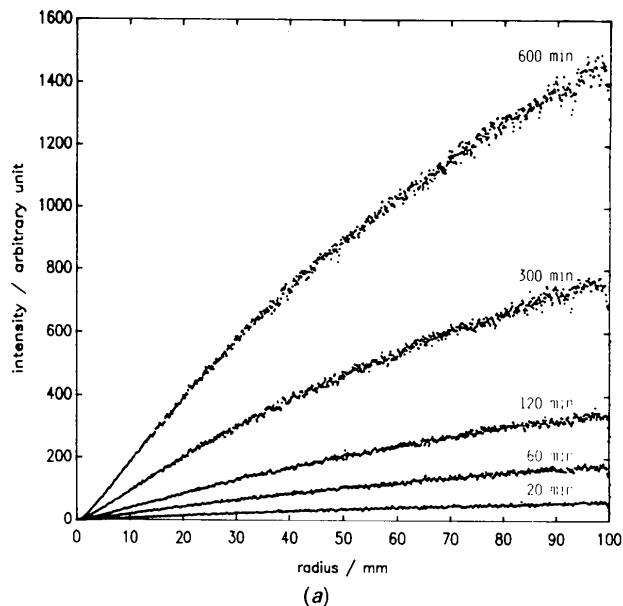

(a)

(b)

Fig. 9. Correction curve for the spiral scanning mode. (a) A uniform exposure was made along a radius of an imaging plate using the radioisotope ^{55}Fe (30 µCi). The latter was mounted on the reader head and traversed repeatedly at lower speed (but high enough to prevent decay), say 100 mm min^{-1}, for specified times, and the intensity along a radius read off. (b) The ratios of each curve to the one for largest exposure (600 min) are given, and it is clear that the correction curve is reliable from 4 to 99 mm.
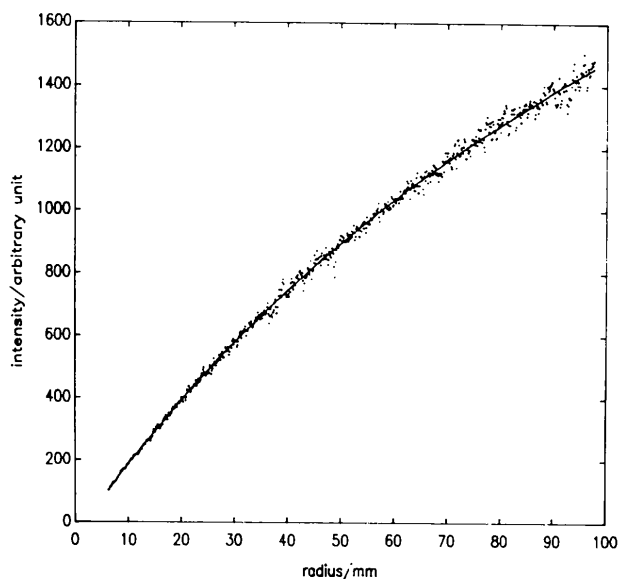

Fig. 10. Profile fitting to the radioisotope scanning data. Formula (2) is fitted to the 600 min exposure data for an area with 5 to 95 mm radius. The parameters k and a are 3·74 × 10^3 and 1·22 × 10^3 respectively.

Table 2. *Experimental conditions and results for the lysozyme crystal*

The lysozyme crystals were prepared from a commercial powder specimen by the vapor-diffusion method (internal: protein 3%w/v, NaCl 0·3 mol l⁻¹, glycerol 7%v/v and external: NaCl 0·9 mol l⁻¹, glycerol 7%v/v).

DIP100

Sample	Hen egg lysozyme, 0·4 × 0·3 × 0·3 mm, $P4_12_12$, $a = b = 79·1$, $c = 37·9$ Å
X-ray source	40 kV, 120 mA (fine focus)
Collimator (φ) (mm)	0·5
Monochromator	Graphite
Camera length (mm)	100
Resolution (Å)	2·0
Rotation axis ω	c^*
Oscillation angle (°)	2·0
No. of films	
Oscillation	23
Still	24

	DATA(I)	DATA(II)
Rotation		
Rotation speed (° s⁻¹)	0·002	0·010
Repetition	1	5
Exposure time (s)		
Oscillation	1000	200 × 5
Still	600	600
No. of reflections		
Observed	9786	7642
Rejected	759	307
Independent	3822	3539
R_{merge} (%)	8·3	8·3

Shell resolution (Å)	No. of reflections Observed	Rejected	Independent	R_{merge} (%)
DATA(I)				
∞–5·0	1090	52	520	8·1
∞–4·0	2154	115	990	8·0
∞–3·5	3234	179	1461	8·1
∞–3·0	4893	367	2258	8·2
∞–2·5	7515	719	3669	8·2
∞–2·0	9818	732	3861	8·3
DATA(II)				
∞–5·0	936	39	453	7·6
∞–4·5	1958	105	910	7·8
∞–3·5	2920	190	1344	8·0
∞–3·0	4453	334	2092	8·0
∞–2·5	6380	539	3247	8·1
∞–2·0	7673	310	3611	8·3

Four-circle diffractometer

X-ray source	40 kV, 120 mA (fine focus)
Collimator (φ) (mm)	0·5
Monochromator	Graphite
Camera length (mm)	400
Scan speed (2θ) (deg min⁻¹)	4
Resolution (Å)	2·5
No. of reflections	
Observed	4633
Rejected	206
Independent	2672
R_{merge} (%)	8·0

Shell resolution (Å)	No. of reflections Observed	Rejected	Independent	R_{merge} (%)
∞–5·0	976	20	538	5·3
∞–4·0	1805	46	1000	6·7
∞–3·5	2562	94	1435	7·5
∞–3·0	3674	204	2119	8·4
∞–2·5	4644	252	2883	8·6

Table 3. *Diffraction experiment for the cytochrome c-553 crystal*

Sample	Cytochrome c-553, *Desulfovibrio vulguris* Miyazaki F, 0·8 × 0·4 × 0·4 mm, $P4_12_12$, $a = b = 42·7$, $c = 103·4$ Å
X-ray source	50 kV, 300 mA (normal focus)
Collimator (φ) (mm)	0·5
Monochromator	Graphite
Camera length (mm)	100
Rotation axis ω	c^*
Rotation speed (° s⁻¹)	0·004
Repetition	3
Oscillation angle (°)	2·5
Exposure time (s)	
Oscillation	625 × 3
Still	300
No. of films	
Oscillation	18 × 2 set
Still	19 × 2 set
No. of reflections	
Observed	19619
Rejected	470
Independent	4292
R_{merge} (%)	6·8

Shell resolution (Å)	No. of reflections Observed	Rejected	Independent	R_{merge} (%)
∞–5·0	283	3	145	3·7
∞–4·0	1399	13	527	4·1
∞–3·5	3014	35	932	4·6
∞–3·0	6235	175	1644	5·3
∞–2·5	12383	353	2995	6·2
∞–2·0	19619	482	4762	6·8

tively higher spatial resolution, one should avoid divergence of the incident X-ray beam. Using a narrow collimator (0·3 mm diameter) with double holes it takes, for a typical protein crystal (say 0·5 mm in each dimension), about 30 min to obtain a large enough number of significant reflections by the oscillation method. As already mentioned, decay of the F centers on the imaging plate means that too long an exposure time is not efficient, *i.e.* an increasing fraction of F centers would suffer from decay. Exposure for 30 min may be the optimum time to obtain one frame of diffraction data. It would appear then that an imaging-plate diffraction apparatus is very useful in protein crystallography if used carefully.

References

JONES, A., BARTELS, K. & SCHWAGER, P. (1977). *The Rotation Method in Crystallography*, edited by U. W. ARNDT & A. J. WANACOTT, pp. 105–117. Amsterdam: North-Holland.
MIYAHARA, J. & KATO, H. (1984). *Jpn. Soc. Appl. Phys.* **53**, 884–890.
MIYAHARA, J., TAKAHASHI, K., AMEMIYA, Y., KAMIYA, N. & SATOW, Y. (1986). *Nucl. Instrum. Methods Phys. Res.* **A246**, 572–578.
NAKAGAWA, A., NAGASHIMA, E., HIGUCHI, Y., KUSUNOKI, M., MATSUURA, Y., YASUOKA, N., KATSUBE, Y., CHIHARA, H. & YAGI, T. (1986). *J. Biochem.* **99**, 605–606.

apparatus of relatively low cost has been described. The high sensitivity and linearity at high intensity for the imaging plate compared with X-ray films are clearly demonstrated. In order to achieve the rela-

SAKABE, N., NAKAGAWA, A., SASAKI, K., SAKABE, K., WATANABE, N., KONDO, H. & SHIMOMURA, M. (1989). *Rev. Sci. Instrum.* **60**, 2440–2441.

SCHWAGER, P., BARTELS, K. & JONES, A. (1975). *J. Appl. Cryst.* **8**, 275–280.

TAKAHASHI, K., MIYAHARA, J. & SHIBAHARA, Y. (1985). *J. Electrochem. Soc.* **132**, 1492.